


Chapter 4

Geospatial and Geophysical Approaches for Assessment of Groundwater Resources in an Alluvial Aquifer of India



Partha Pratim Adhikary , S. K. Dubey, Debashis Chakraborty,
and Ch. Jyotiprava Dash

Abstract Western Delhi is a peri-urban area and mainly produces cash crops like vegetables. For round the year vegetable production, the farmers in this area depend on groundwater for irrigation. Thus, widespread groundwater withdrawal for intensive vegetable cultivation is the primary cause of depletion of groundwater quantity in this part of Delhi. To understand sub-surface geologic condition and to assess groundwater availability, geophysical imaging of the sub-surface was carried out. Groundwater potential zones were found at 18–30 m below ground level, and the quality of groundwater seems to be of moderate to poor because of low resistivity values in the water potential zones. Geospatial mapping of the resistivity values of different sub-surface layers identified the geological formations like coarse fragments, clay, calcite and other formations. Longitudinal Unit Conductance (S value) and Transverse Unit Resistance (T value) and their combinations are found effective to identify groundwater potentiality. Geospatial maps prepared by ordinary kriging interpolation method indicated that 20.2% of the area has potential to get good quality groundwater. But these areas are scatteredly distributed at the east, west, and north side of west Delhi. The aquifer of the southern part of the study area showed low resistivity formation, which indicates groundwater pollution. The infiltrations of

P. P. Adhikary
ICAR-Indian Institute of Water Management, Bhubaneswar, India

S. K. Dubey (✉)
ICAR – Indian Agricultural Research Institute, New Delhi, India

ICAR – Indian Institute of Soil and Water Conservation, Research Centre, Agra, Uttar Pradesh,
India

D. Chakraborty
ICAR – Indian Agricultural Research Institute, New Delhi, India

Ch. J. Dash
ICAR – Indian Institute of Soil and Water Conservation, Research Centre, Koraput, Odisha,
India

highly polluted Najafgarh drain water and fertilizer laden surface water and their subsequent movements to the aquifer are mainly responsible for this. The study will help to identify the hotspots for periodic monitoring of groundwater quality. The study also suggests the directions of future research works for scientific development and management of groundwater resources in west Delhi.

Keywords Delhi · Geophysical imaging · Groundwater potentiality · Longitudinal Unit Conductance · Resistivity · Transverse Unit Resistance

4.1 Introduction

Monsoonal uncertainty and excessive withdrawal of groundwater over recharge are the main reasons of lowering of water table and also deterioration of groundwater quality in many parts of India (Adhikary et al. 2009). The problem is more acute in the alluvial aquifers where, nowadays, good quality water is primarily available in the deeper aquifers. The main geological formations in alluvial areas of North India are the deposition of weathered materials carried out by the rivers and wind; thus a regolith, normally produced by ex situ weathering, is highly deep. Hydro-geologically, the porosity of the weathered regolith is generally high and stores high amount of water; but it can show low permeability because of high clay content. Therefore, to get high water yield for a long duration, the bore well needs to be penetrated a large thickness of regolith. The farmers in the alluvial zones have the tendency to drill bore wells haphazardly without knowing the water bearing potential of the aquifer, resulting the failure of the bore wells. This may sometime increase the debt burden of the farmers.

Therefore, to help the farmers in the alluvial zone, proper appraisal of groundwater in terms of quantity and quality needs to be done. This is also needed to plan and manage groundwater scientifically for its multiple uses like irrigation, drinking, domestic and industrial uses, recreation, etc. In one hand, groundwater quality deterioration is generally linked to some point source activity like municipal and industrial waste depositions and non-point source activity like spraying of pesticides and fertilizers to the field in excess (Adhikary et al. 2010), and on the other hand, the quantity of groundwater available for different use is linked with indiscriminate withdrawal of groundwater for agriculture owing to no or very low electricity charge. The extent of groundwater withdrawal changes from year to year and season to season based on various issues and thus needs proper investigation for its efficient utilization.

The aquifer systems are very complex and the groundwater-related problems are very site specific. Therefore, a single approach for scientific evaluation and proper management of groundwater may not be sufficient and thus calls for an integrated

approach (Adhikary et al. 2014a, 2015a). To understand groundwater quality, the widely used method is hydro-chemical method (Adhikary et al. 2009, 2014b; 2015b; Prasanna et al. 2011). Geophysical technique, on the other hand, can easily assess and monitor spatio-temporal change of groundwater resources. It is a rapid, non-destructive, and cost-effective technique to monitor groundwater system as compared to conventional hydro-chemical technique (Adhikary et al. 2015a). Geophysical technique is the ensemble of four techniques, namely, geo-electrical, seismic, gravimetric, and electromagnetic. Among these, geo-electrical technique is the widely used technique to monitor aquifer characteristics (Skuthanet et al. 1986). Dependability and cost-effectivity are the two important issues of geo-electrical technique which have led to its widespread use in groundwater quality management (Mazac et al. 1987; Skuthan et al. 1986; Al Garni 2011; Adhikary et al. 2015a).

The zones of poor groundwater quality can be effectively monitored by geophysical imaging technique (Rao et al. 2011). It is the two-dimensional visualization of the variation of sub-surface resistivity and can be created by inverting the simultaneous measurement of many individual resistance (Adhikary et al. 2015a). Not only two-dimensional imaging, three-dimensional resistivity imaging is also widely used to monitor aquifer characteristics and groundwater pollution (Ustra et al. 2012). Geophysical imaging technique has widely been used for mapping of sub-surface configurations (Griffiths and Barker 1993; Loke and Barker 1996). The mapping of groundwater pollution plumes in the aquifer and their spatial and temporal movements can also be assessed by using geophysical imaging technique (Adhikary et al. 2015a).

For mapping of groundwater resources, the geospatial interpolation approach may be either deterministic, like inverse distance weighting (Varouchakis and Hristopulos 2013) and radial basis function (Arslan 2014) or stochastic, like ordinary kriging (Sun et al. 2009; Adhikary et al. 2010, 2012; Adhikary and Biswas, 2011; Arslan 2014), indicator kriging (Adhikary et al. 2011), and universal kriging (Sun et al. 2009; Adhikary and Dash 2017). But the widely used geospatial interpolation of groundwater resources is ordinary kriging (OK). OK was used by Prakash and Singh (2000) to determine optimum number of observation wells for monitoring of groundwater level spatially. Adhikary et al. (2015b) have used geostatistics for sustainable management of groundwater resources. OK has widely been used to optimize the groundwater level monitoring network and also to improve the quality of the monitored data (Theodossiou and Latinopoulos 2006). Ahmadi and Sedghamiz (2008) used OK to establish spatial and temporal structure of water level spatial variation. The application of OK to understand the spatial structure of water table data under non-uniformly spaced observation wells has been reported by Nikroo et al. (2010) in Iran. In a study in India, OK has been used to develop water table management network in an area where sufficient monitoring well is absent (Dash et al. 2010).

Thus, geophysical imaging along with ordinary kriging spatial interpolation technique has the capability to systematically assess and monitor the groundwater resources in a cost-effective way. The efficacy of these techniques has been

demonstrated in the southern part of Najafgarh block, which is situated at west Delhi, bordering Haryana state of India, which is a peri-urban area where huge amount of groundwater is being withdrawn for agricultural purpose. In this block, overexploitation of groundwater for growing mainly vegetable crops has been reported as the main cause of lowering of water table (CGWB 1996) and increasing of groundwater salinity (Adhikary et al. 2010, 2012, 2015c). In this context, geophysical imaging can become a handy tool to quantify the groundwater resources in this area. Therefore, the present study has been undertaken to assess the present status of groundwater through geophysical imaging of the sub-surface and subsequent spatial interpolation of groundwater quality using ordinary kriging interpolation technique.

4.2 Materials and Method

4.2.1 *The Study Area*

Delhi is a small state located at the juncture of the Indo-Gangetic plain and Aravalli range. It lies between north latitudes $28^{\circ}24'17''$ and $28^{\circ}53'00''$ and east longitudes $76^{\circ}50'24''$ and $77^{\circ}20'37''$. The location of the study area is the west side of Delhi state, that is the southern part of Najafgarh block. It lies between north latitude of $28^{\circ}30'14''$ and $28^{\circ}39'45''$ and east longitude of $76^{\circ}50'24''$ and $77^{\circ}02'15''$ with area-wise coverage of about 189 km^2 (Fig. 4.1). The Najafgarh drain flows along the south and east boundary, and Kultana Chhudani Bupania drain flows along the north boundary of the study area. It is surrounded by Jhajjar district and Nangloi block in the north, East Najafgarh block in the east, Gurgaon district in the south, and Jhajjar district in the west.

4.2.2 *Physiography, Relief, and Drainage*

Three types of physiographic units are found in the study area. They are undulating plains, piedmont plains, and the Aravalli ridge. Undulating plains are formed from the fluvio-aeolian deposits coming from Yamuna River and Rajasthan desert. In some areas, colluvial deposits from the Aravalli ranges also form the undulating plains. Piedmont plains are formed at the foothills of the Aravalli range, and these plains are modified by aeolian deposits or by fluvian deposits. The Aravalli ridge is a long, narrow continuation of the Aravalli range and dissects Delhi state from south to north.

The topography of Delhi is undulating in nature with an average elevation of 227 m above mean sea level. The elevation ranges between 198 and 326 m above mean sea level, and the average slope is from south-west to north-east direction. The drainage is important to remove excess water from the land surface as well as

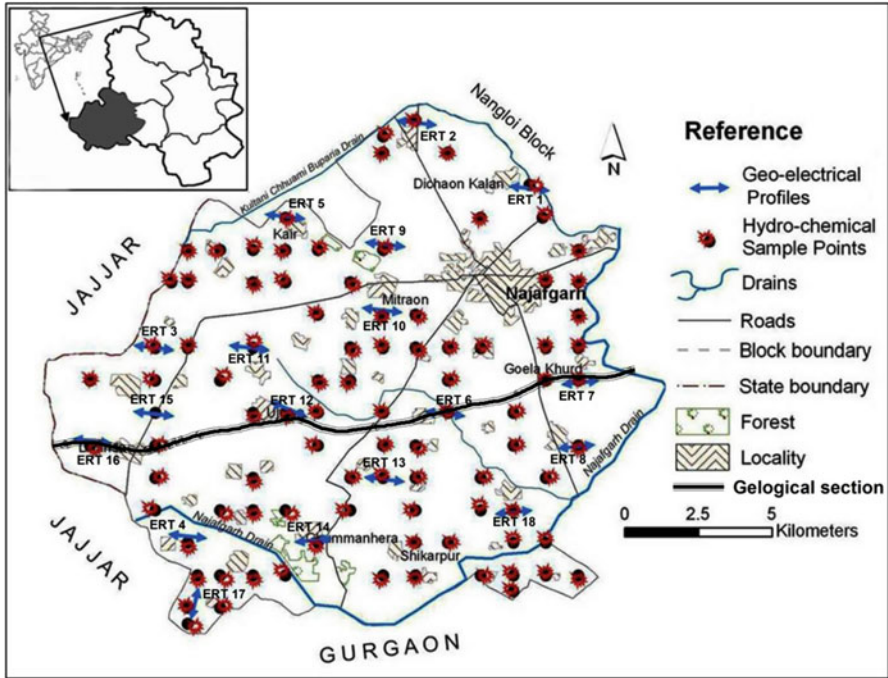


Fig. 4.1 Study area map showing the location of the geophysical survey points and hydro-chemical sampling points

sub-surface. With the drainage water, salt and other harmful chemicals are also being removed from the productive fertile land. The Najafgarh drain, originated from Najafgarh *jheel*, is the main drainage system of the area forming the southern boundary. Kultana Chhudani Bupania drain forms the northern boundary of the study area and drains the water to the Najafgarh drain, which ultimately meets the Yamuna River. A small *nala* originates from the western part bifurcate the study area and meets the Najafgarh drain.

4.2.3 Climate

The study area belongs to sub-tropical semi-arid climatic condition. In this area, dry hot summer and cold winter are the characteristic features. The average annual temperature of the study area is 25.6 °C. Mean maximum temperature is nearly 45 °C observed in the month of June, whereas mean minimum is nearly 7 °C observed in the month of January. Rainfall is unimodal, and monsoon is the main rainy season when more than 80% of rainfall occurs. According to IMD (1991), the long-term average annual rainfall of the area is 611.8 mm occurring in 27 rainy days.

During summer season the average relative humidity ranges between 20 and 30%, whereas during monsoon season the same varies between 62.5 and 75%.

4.2.4 Soils and Geology

The USDA Soil Taxonomy is coarse loamy, mixed, hyperthermic Typic Haplustepts. The soil texture is sandy loam to loamy sand. In some pockets, loam-textured soil has also been found. The soil series is Palam series having the characteristic of very deep, yellowish-brown alluvial material. Calcium carbonate concretions are also present in the sub-soil. Quartzite sandstone and mica schist are the main lithology of the study area. At the foothills piedmont plain is found and formed from the deposition of alluvial materials. Granite, schist, and ferruginous lime quartzite are the predominant minerals from which the surface soil is developed. Epidote-zoisite (32–50%), hornblende (17–34%), iron oxide (10–20%), garnet-kyanite-zircon-titanite (9–14%), tourmaline (1–3%), and mica (1–2%) are the dominant minerals of fine sand (Sen 1952).

4.2.5 Natural Vegetation and Land Use

Dry deciduous trees are the types of natural vegetation found in the study area. The common vegetations comprise Babool (*Acacia arabica*), Dhak (*Butea monosperma*), Doob (*Cynodon dactylon*), Jand (*Prosopis cineraria*), Jharberi (*Ziziphus nummularia*), Kikar (*Acacia catechu*), Moonj (*Sacharum munja*), Neem (*Azadirachta indica*), Pipul (*Ficus religiosa*), and Shisham (*Dalbergia sissoo*). Agriculture is the dominating land use comprising 75% of the study area. Forests habitats, ponds, roads, etc. are the other land uses. Pearl millet, chick pea, and green gram are grown in the rainy season, and wheat and mustard are cultivated during the winter season. Now widespread cultivation of vegetables is the main agricultural practice. Irrigation by deep tube well is a common practice. Sprinkler and drip irrigation are also being practiced by few farmers.

4.2.6 Geophysical Imaging Investigation

Geophysical imaging was done by using Lund imaging technique. This imaging technique was primarily based on resistivity measurement of the sub-surface. Resistivity meter is the instrument which is used to measure sub-surface resistivity. The principle involves two current and two potential electrodes inserted into soil along a

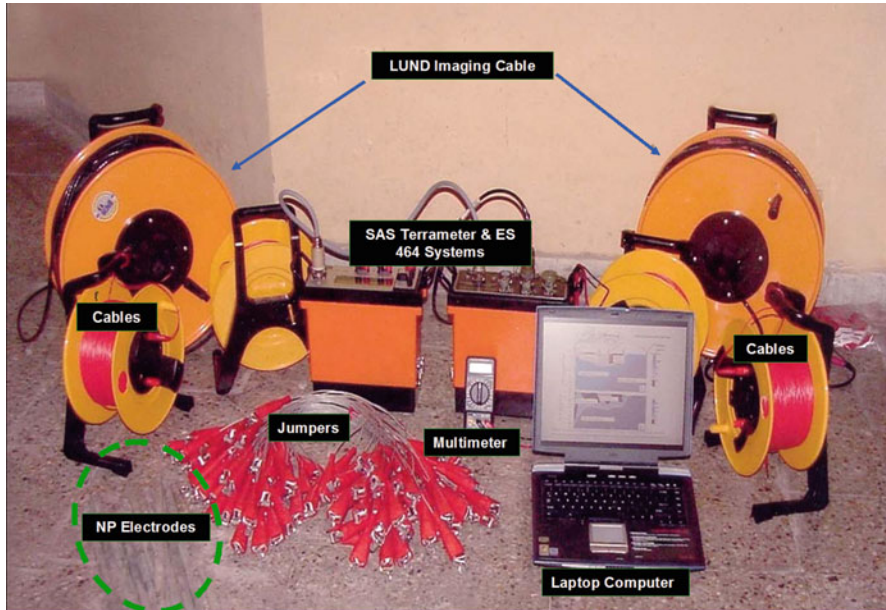


Fig. 4.2 Geophysical instruments (Lund Imaging System) for groundwater survey

straight line with some particular distance apart. The potential difference between the potential electrodes is measured and interpreted as a result of the controlled current that is passed through the current electrodes. Depending on actual electrode configuration, the separation distances between the electrodes are changed. By this way a series of apparent resistivity (ρ_a) was obtained, which is the resistivity of an equivalent homogeneous medium where the same current is used to produce the same potential drop (Bhattacharya and Patra 1968). The geological matrixes of the sub-surface govern the resistivity value. Generally, the compact rock shows very high resistivity value, and the fractured rocks with water shows very low resistivity value (Verma *et al.* 1980).

In the present study, Lund Imaging System was used where separation distance between two electrodes was increased with each successive pass. By increasing the electrode spacing, the depth of penetration has been increased. The equipment used for Lund imaging are shown in Fig. 4.2.

The lateral and vertical apparent resistivity variation of the underlying sub-surface matrix was used to make a 2D pseudo-section. It was constructed by plotting the apparent resistivity on vertical section at a depth equivalent to the median depth of investigation (Edwards 1977). The data are contoured to form a pseudo-section. RES2DINV software was used to determine a 2D resistivity model of sub-surface for the data obtained from electrical imaging survey (Griffiths and Barker, 1993). A forward modeling subroutine was used to calculate the apparent

resistivity values, and a non-linear least squares optimization technique was used for the inversion routine (De Groot_Hedlin and Constable 1990; Loke and Barker 1996). Inversion routine used by the program is based on the smoothness constrained in Least Squares method (De Groot_Hedlin and Constable 1990; Sasaki 1992).

4.2.7 Interpretation of Geophysical Data

The data coming out of geophysical imaging was interpreted to calculate the thickness and the resistivity of different sub-surface layers. The apparent resistivity data was interpreted for this purpose using Schlumberger configuration (Dorbin 1960) from the following formula:

$$\rho_a = \frac{\frac{\pi}{4} \times \frac{(e^2 - p^2)}{p^2}}{\frac{V}{I}} \quad (4.1)$$

where “e” is the distance between current electrodes and “p” is the distance between potential electrodes.

For better assessment of potential groundwater zones in the study area along with true resistivity data, Dar Zarrouk parameters S (Longitudinal Unit Conductance) and T (Transverse Unit Resistance) were calculated. True resistivity data (combining resistivity and thickness) of each geophysical image was interpreted, and the corresponding values of longitudinal unit conductance (S) and transverse unit resistance (T) parameters for each geophysical image were computed. The formula to calculate Dar Zarrouk parameters are given below:

For a sequence of horizontal, homogeneous, and isotropic layers of resistivity ρ_i and thickness h_i , where S and T are defined by:

$$S = \sum_{i=1}^n \frac{h_i}{\rho_i} \quad (4.2)$$

and

$$T = \sum_{i=1}^n h_i \times \rho_i \quad (4.3)$$

where ρ_i is the resistivity of a homogeneous and isotropic layer, h_i is the thickness of a homogeneous and isotropic layer, and n is the number of layers.

4.2.8 Geospatial Approach in Development of Spatial Variability Models

The spatial variability map of the sub-surface configuration can be visualized through apparent resistivity contours. These iso-resistivity contours of various layers were interpolated through ordinary kriging technique. Kriging is the mostly used spatial interpolation technique because of its flexibility to understand the spatial autocorrelation of the variables. It can give option to estimate interpolation error. Thus, we can get estimation accuracy and reliability of the spatial distribution of the variable. The spatial dependence can be quantified from semivariogram (Burgess and Webster 1980). It is the mean square variability between two neighboring points of distance h as shown in Eq. (4.5):

$$\gamma(h) = \frac{1}{2N(h)} \sum_{i=1}^{N(h)} [z(x_i + h) - z(x_i)]^2 \tag{4.4}$$

where $\gamma(h)$ is the semivariogram expressed as a function of the magnitude of the lag distance or separation vector h between two points, $N(h)$ is the number of observation pairs separated by distance h , and $z(x_i)$ is the random variable at location x_i .

The experimental semivariogram $\gamma(h)$ can be fitted in a theoretical model such as spherical, exponential, linear, or Gaussian to determine three parameters, such as the nugget (c_0), the sill (c), and the range (A_0). These models are defined as follows (Issaks and Srivastava 1989):

Spherical model:

$$\begin{aligned} \gamma(h) &= c_0 + \left[1.5 \left(\frac{h}{A_0} \right) - 0.5 \left(\frac{h}{A_0} \right)^3 \right] & h \leq A_0 \\ \gamma(h) &= c_0 + c, & h > A_0 \end{aligned} \tag{4.5}$$

Exponential model:

$$\gamma(h) = c_0 + c \left[1 - \exp \left(-3 \frac{h}{A_0} \right) \right] \tag{4.6}$$

Gaussian model:

$$\gamma(h) = c_0 + c \left[1 - \exp \left[- \left(\frac{3h}{A_0} \right)^2 \right] \right] \tag{4.7}$$

Linear model:

$$\gamma(h) = c_0 + h\left(\frac{c}{A_0}\right) \tag{4.8}$$

Based on R2 and RSS, we determine which model needs to be used.

4.3 Result and Discussion

4.3.1 Geophysical Imaging

Eighteen profiles of geophysical imaging of the sub-surface were carried out at the southern part of Najafgarh block of Delhi. The resulting geophysical images for groundwater are presented from Figs. 4.3, 4.4, 4.5, 4.6, 4.7, 4.8, 4.9, 4.10, 4.11, 4.12, 4.13, 4.14, 4.15, 4.16, 4.17, 4.18, 4.19, and 4.20.

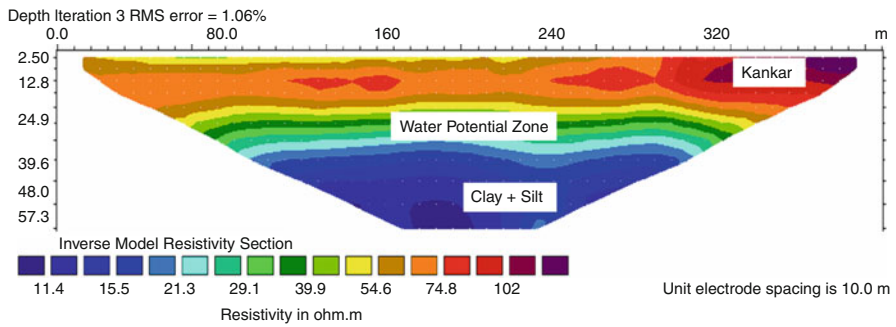


Fig. 4.3 Geophysical image of the sub-surface obtained at Dichaon Kalan village of Delhi showing various geological layers and groundwater potential zones (Profile 1)

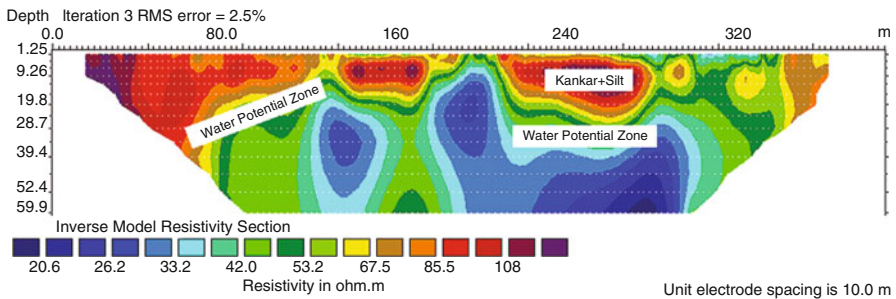


Fig. 4.4 Geophysical image of the sub-surface obtained at Jharoda Kalan village of Delhi showing various geological layers and groundwater potential zones (Profile 2)

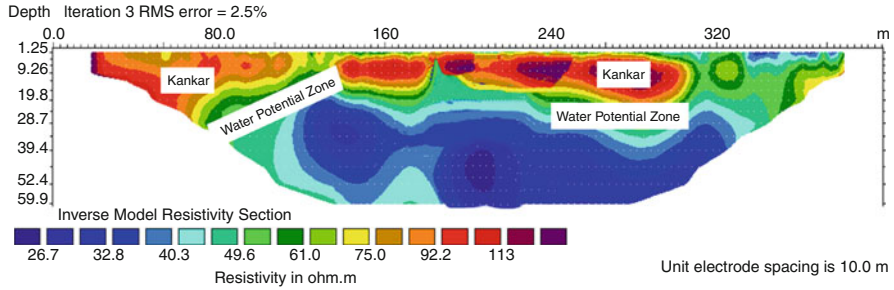


Fig. 4.5 Geophysical image of the sub-surface obtained at Bagargarh village of Delhi showing various geological layers and groundwater potential zones (Profile 3)

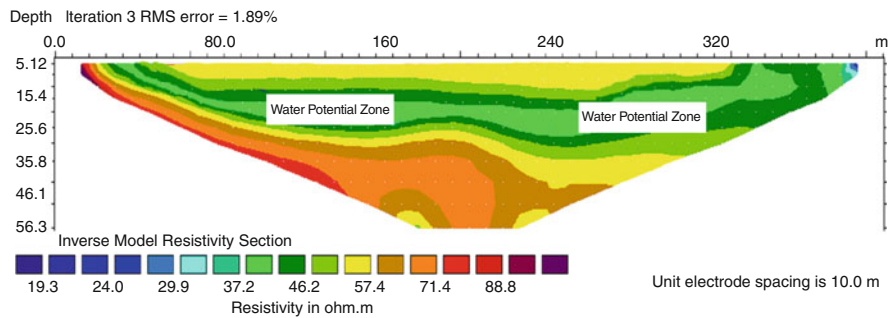


Fig. 4.6 Geophysical image of the sub-surface obtained at Goela Khurd village of Delhi showing various geological layers and groundwater potential zones (Profile 4)

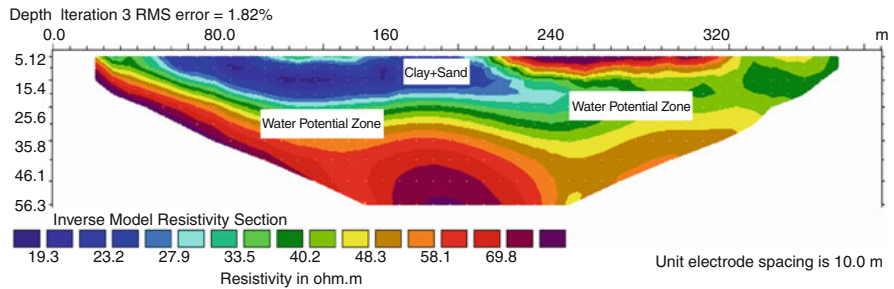


Fig. 4.7 Geophysical image of the sub-surface obtained at Kair village of Delhi showing various geological layers and groundwater potential zones (Profile 5)

4.3.1.1 Geophysical Imaging Through Profile 1

In the south west side of Dichaon Kalan village, the first geophysical imaging was done. The first electrode to get the sub-surface geophysical profile was inserted just side of a road, and the other electrodes went through an agricultural field. The value of resistivity ranges between 10 and 130 ohm-m. Figure 4.3 indicates that at the

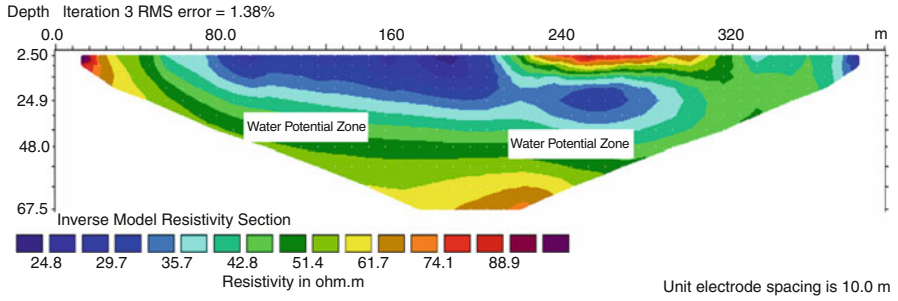


Fig. 4.8 Geophysical image of the sub-surface obtained at Pindwala Kalan village of Delhi showing various geological layers and groundwater potential zones (Profile 6)

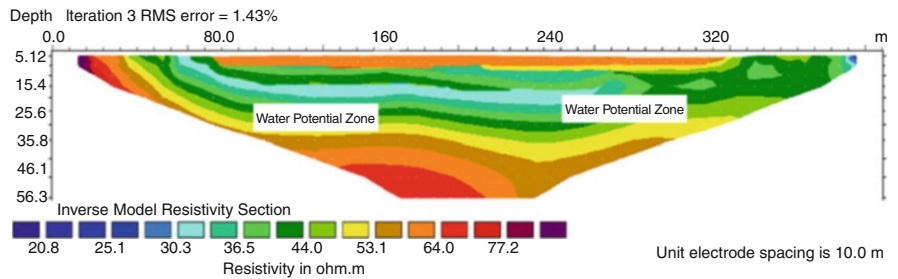


Fig. 4.9 Geophysical image of the sub-surface obtained at Qazipur village of Delhi showing various geological layers and groundwater potential zones (Profile 7)

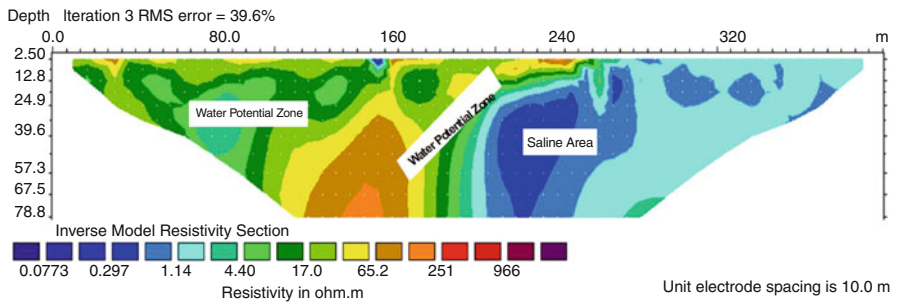


Fig. 4.10 Geophysical image of the sub-surface obtained at Daurala village of Delhi showing various geological layers and groundwater potential zones (Profile 8)

upper depth kankar is the predominating geological material with a resistivity value of 60–115 ohm-m. The absence of any bed rock is also evidenced from this profile. At a lower depth (more than 40 m bgl) low resistivity materials are found which may be made up of clay and silt. Within the sub-surface profile, the geological layers are distinctly separated from each other in the vertical direction. In the horizontal direction the variation of resistivity is very low. This is a clear indication of alluvial

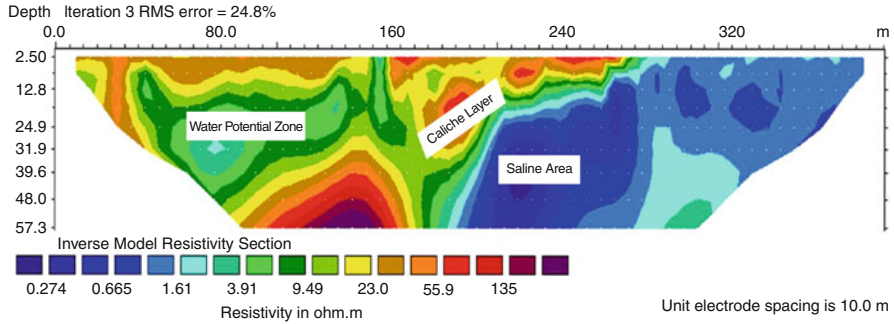


Fig. 4.11 Geophysical image of the sub-surface obtained at Ghalibpur village of Delhi showing various geological layers and groundwater potential zones (Profile 9)

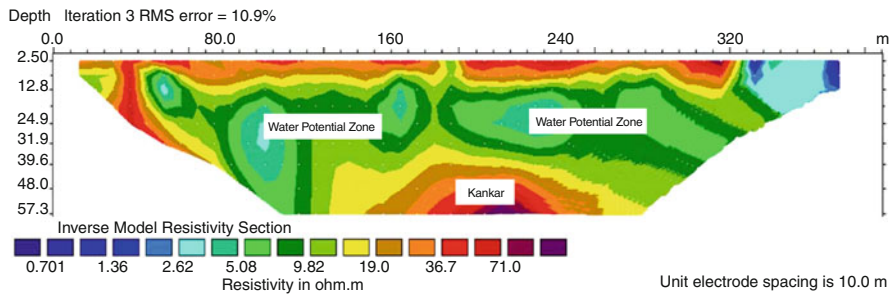


Fig. 4.12 Geophysical image of the sub-surface obtained at Mitraon village of Delhi showing various geological layers and groundwater potential zones (Profile 10)

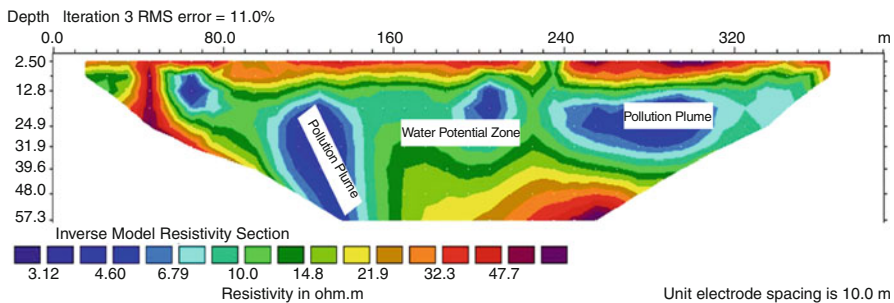


Fig. 4.13 Geophysical image of the sub-surface obtained at Jaffarpur Kalan village of Delhi showing various geological layers and groundwater potential zones (Profile 11)

deposits under different geological era, as the area is coming under the flood plain of River Yamuna. Groundwater potential zones are expected within the depth of 20–30 m below ground level (bgl) where the resistivity value varies between 28 and 48 ohm-m.

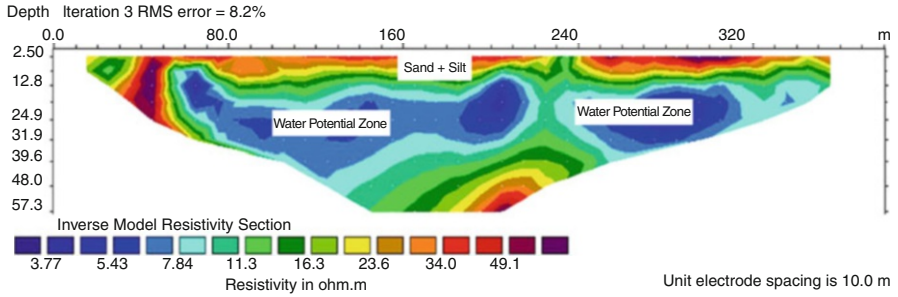


Fig. 4.14 Geophysical image of the sub-surface obtained at Ujwah village of Delhi showing various geological layers and groundwater potential zones (Profile 12)

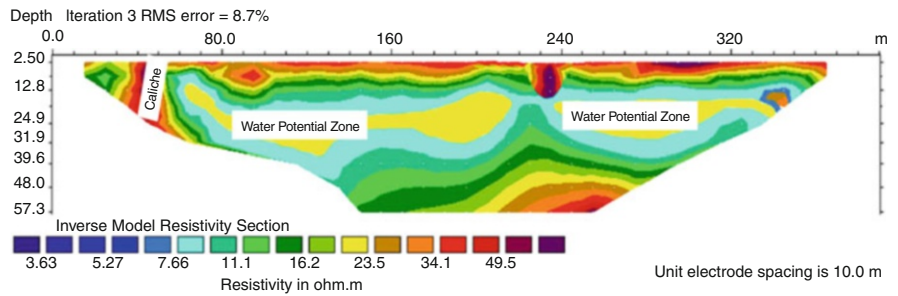


Fig. 4.15 Geophysical image of the sub-surface obtained at Surkhpur village of Delhi showing various geological layers and groundwater potential zones (Profile 13)

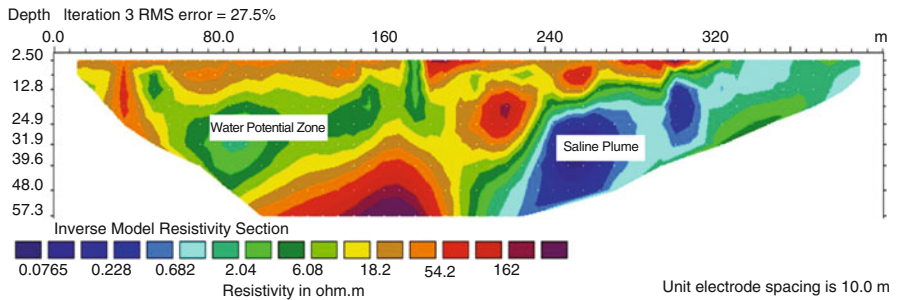


Fig. 4.16 Geophysical image of the sub-surface obtained at Ghummanhera village of Delhi showing various geological layers and groundwater potential zones (Profile 14)

4.3.1.2 Geophysical Imaging Through Profile 2

The second geophysical imaging was done at Jharoda Kalan village of Delhi. The entire sub-surface resistivity profile run through a farmer’s field situated at the side of a village road (Fig. 4.4). The value of resistivity ranges between 15 and 140 ohm-m. The upper part of the sub-surface with the depth ranging from 2 to

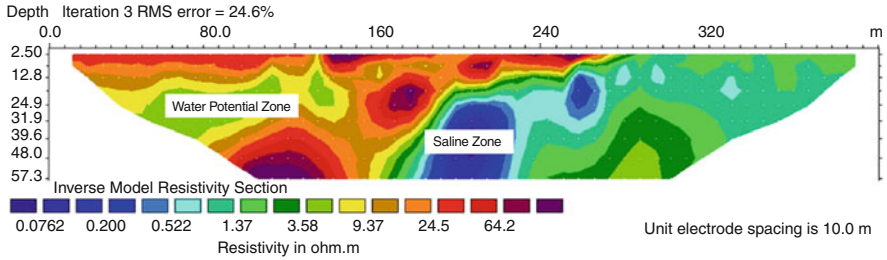


Fig. 4.17 Geophysical image of the sub-surface obtained at Chhawala village of Delhi showing various geological layers and groundwater potential zones (Profile 15)

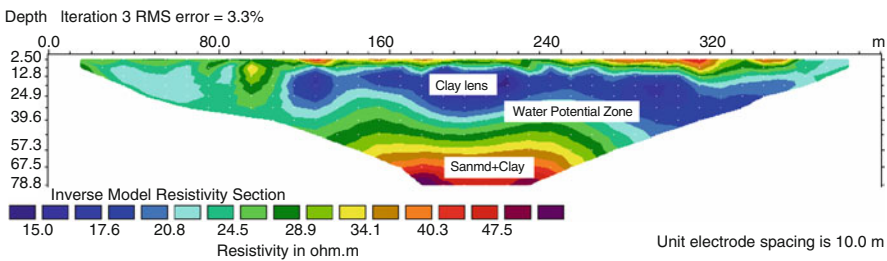


Fig. 4.18 Geophysical image of the sub-surface obtained at Hasanpur village of Delhi showing various geological layers and groundwater potential zones (Profile 16)

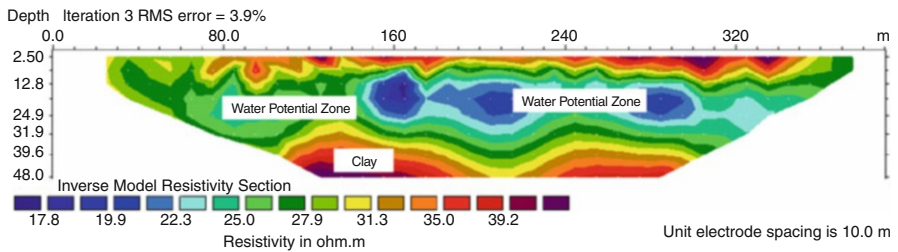


Fig. 4.19 Geophysical image of the sub-surface obtained at Dhansa village of Delhi showing various geological layers and groundwater potential zones (Profile 17)

15 m bgl mainly comprises course materials like kankar and kankar plus silt. The resistivity of this zone is somewhat high and ranges between 100 and 140 ohm-m. This kankar layer is predominantly found at the start of the profile and up to 300 m from the starting point. After that the sub-surface configuration changes and it becomes slightly finer. Clay lenses are observed in between 200 and 300 m away from the starting point and at a depth of 40–50 m bgl. Water bearing layer may be expected at a depth of 20–30 m bgl, and the resistivity of this layer varies between 32 and 53 ohm-m. This profile is very much helpful to identify the location of a potential bore hole.

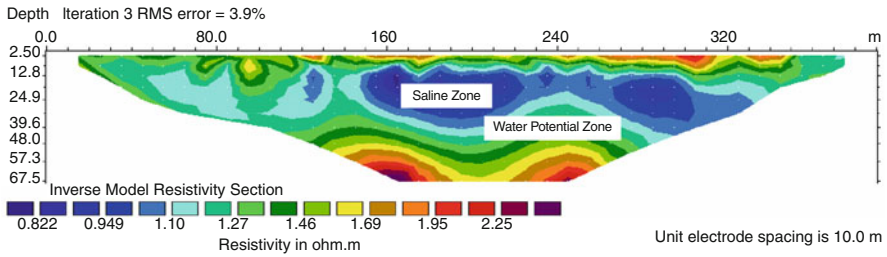


Fig. 4.20 Geophysical image of the sub-surface obtained at Kanganheri village of Delhi showing various geological layers and groundwater potential zones (Profile 18)

4.3.1.3 Geophysical Imaging Through Profile 3

The geophysical image along with profile 3 was obtained near the side of a monument in the village Bagargarh of Delhi and partially along the road side (Fig. 4.5). The value of resistivity ranges between 15 and 140 ohm-m and showing wide vertical and horizontal variation. The coarse textured materials are dominant at the upper part of the sub-surface which mainly consist of kankar. Between 13 and 28 m bgl, water bearing formation is expected, and beyond that the presence of low resistivity zone is an indicator of the dominance of clay, kankar, and silt. The presence of clay lens at 30 m to 40 m depth is indicative of the formation of a confined aquifer beneath 40 m in this area.

4.3.1.4 Geophysical Imaging Through Profile 4

The geophysical image along profile 4 has been obtained at a vegetable field in the Goela Khurd village of Delhi (Fig. 4.6). The vegetable field was located just side of a farm road. The value of resistivity ranges between 15 and 100 ohm-m. The horizontal variation of resistivity is insignificant in this case, and the vertical variation is also very low. The groundwater may be available at a depth of 14 m to 25 m bgl. High resistivity values below the aquifer indicate that aquifer may be overlaying on a calcitic bed rock.

4.3.1.5 Geophysical Imaging Through Profile 5

The geophysical image along profile 5 was obtained from an orchard field located at the south-eastern part of the village Kair (Fig. 4.7). The arrangement of the profile is along with a road. The resistivity values of the sub-surface range between 17 and 91 ohm-m. In the sub-surface, the upper part is dominated with clay and sand. The expected groundwater depth is 16 to 31 m below ground level. The resistivity value of the water bearing layers indicates the presence of good quality groundwater in this area. The hydro-chemical parameters also support the fact. At a deeper depth of more

than 40 m below ground level, high resistivity vale has been observed. The presence of dolomite and calcite at deeper layer may be the reason for high resistivity of this zone. The presence of high calcium and magnesium ion in the groundwater of deep tube wells also supports this fact.

4.3.1.6 Geophysical *Imaging Through Profile 6*

The geophysical image along profile 6 was obtained from a government field lying along the main road which is situated just eastern part of Pindwala Kalan village (Fig. 4.8). The arrangement of the profile is also along the main road. The resistivity value of the sub-surface geological materials ranges between 18 and 110 ohm-m. At the upper part of the sub-surface geologic material, the resistivity varies widely in the horizontal direction. In the vertical direction the resistivity value increases gradually. Low resistivity at the upper part of the vadose zone indicates that there may be accumulation of soil moisture at this part of the vadose zone. This may be because of capillary movement of water to the soil surface from the underneath saturated zone. Water bearing layers are expected at a depth of 25–40 m bgl. The groundwater quality in this area is good to moderate as evidenced from the resistivity value of the water bearing layers. The hydro-chemical data is also indicative of the same.

4.3.1.7 Geophysical *Imaging Through Profile 7*

The geophysical image along profile 7 was laid at the outside boundary of an orchard situated at the southern portion of the village Qazipur (Fig. 4.9). The arrangement of the profile is along the direction of the orchard but perpendicular to the main road. The value of resistivity in this profile ranges from 14 ohm-m to 102 ohm-m. The geo-electrical layers in this profile are quite parallel to each other, and more than 45 m of depth below ground level there is a material of high resistivity, which may be the bed rock made up of lime stones. Presence of high concentration of calcium and bicarbonate in the groundwater is an indicative of the same. Water potential zone is expected at a depth of 16 to 30 m bgl. At the surface layer, the high resistivity value is an indication of the presence of coarse textured soil like sandy soil. The resistivity value of the water potential zone shows that the quality of groundwater is good to moderate and which is also evidenced from the hydro-chemical data.

4.3.1.8 Geophysical *Imaging Through Profile 8*

The geo-electrical image along profile 8 was obtained from a farmer's field lying along the village road situated at the western part of the village Daurala (Fig. 4.10). The arrangement of the profile is along the direction of the road. There is a wide variation of resistivity in this profile both for horizontal and vertical direction. The range of resistivity is also very high, ranging from 0.0773 ohm-m to 250 ohm-m. The

potential water bearing zone is expected at a depth of 15 to 35 m below ground level. The resistivity values of the sub-surface features are clearly revealing that the groundwater is saline in nature and the level of salinity is increasing after 200 m from the start of the profile. The hydro-chemical data are also confirming the result. An interesting finding from the image is that the pollution plume is migrating from right side of the profile to the left side. In real sense, the direction is toward the depression area of the Najafgarh drain.

4.3.1.9 Geophysical Imaging Through Profile 9

The geo-electrical image along profile 9 was obtained from the western side of a horticultural farm situated at the eastern part of the village Ghalibpur (Fig. 4.11). The resistivity variations of different layers are very complex, and for both the horizontal and vertical direction a wide variation of resistivity has been found. The value of resistivity varies from 0.274 ohm-m to 210 ohm-m. The very low resistivity value is an indication of salinity, and the hydro-chemical data are also showing that the groundwater is of highly saline in nature. Water bearing layers are expected at a depth of 20 to 40 m below ground level. At a distance of 220 m from the start of the profile, a highly saline zone is expected. The abrupt change of high resistivity near the surface and the vadose zone is an indication of the presence of caliche (CaCO_3) layer in the sub-surface. This is quite possible in the sub-surface layers of the arid and semi-arid regions of India.

Geophysical Imaging Through Profile 10

The geophysical image along profile 10 was laid in a farmer's field just side of the main road situated at the south-western part of the village Mitraon (Fig. 4.12). The resistivity value varies from 0.701 ohm-m to 110 ohm-m, and the variation is showing a very clear trend. A good amount of groundwater can be expected at a depth of 15 m to 40 m below ground level. The groundwater quality at Mitraon village can be expected as moderate to poor because of very low resistivity of the water potential zone. Hydro-chemical investigation supports this result where moderate groundwater quality is observed. At the upper part of the vadose zone and at a depth more than 50 m, moderate to high resistivity value is observed. Coarse textured materials like sand and *kankar*'s presence at those layers may be responsible for this high resistivity value.

4.3.1.10 Geophysical Imaging Through Profile 11

The geophysical image along profile 11 was laid on a farmer's field cultivated with seasonal vegetables just side of a shallow tube well situated at the northern part of the village Jaffarpur Kalan (Fig. 4.13). The profile is along the north-south direction.

The resistivity of the sub-surface varies from 1.02 to 72 ohm-m, and the degree of variation is very high in both the horizontal and vertical directions. Groundwater can be available in the layers situated at a depth of 25 to 40 m below ground level. The groundwater quality is expected to be poor because of very low resistivity of the water potential zone. The same conclusion was drawn from the results of hydro-chemical investigations. Very low resistivity zones within the water bearing layers may be the pollution slugs having high electrical conductivity. A layer of high resistivity was observed near the surface. This indicates the presence of coarse fragments like sand and *kankar* in that layer.

4.3.1.11 Geophysical Imaging Through Profile 12

The geophysical image along profile 12 was also laid on a farmer's field by the side of a village road at the eastern part of the village Ujwah (Fig. 4.14). The arrangement of the profile is along the east-west direction. The profile is also similar to the previous one that is like Jaffarpur Kalan. The resistivity value of this profile varies between 1.54 and 74 ohm-m. The value of resistivity varies more along the vertical direction, and along the horizontal direction it remains somewhat consistent. The availability of water bearing layers can be expected at a depth of 15 to 40 m below ground level. The groundwater quality is poor because of very low observed resistivity of the water bearing layers. The hydro-chemical investigations also support this result. A high resistivity value near the surface is the result of presence of coarser material like *kankar* in that layer. A similar high resistivity value has also been observed at the lower depth, which may also indicate the presence of dolomite and calcite bed rock.

4.3.1.12 Geophysical Imaging Through Profile 13

The geophysical image along profile 13 was laid on a field at the eastern side of a farm house which is situated at the eastern part of the village Surkhpur (Fig. 4.15). The arrangement of the profile is along the east-west direction. The resistivity value of the sub-surface configuration varies from 2.33 to 73 ohm-m. The geological layers bearing water may be situated at a depth of 15 to 37 m below ground level. The groundwater quality is poor as indicated by the very low resistivity of the water bearing layers in the sub-surface, and this is also confirmed from the hydro-chemical data. A high resistivity value near the surface is an indication of presence of coarse fragments like sand and silt in that layer. A layer of calcium carbonate (caliche layer) has been observed at a horizontal distance of 40 m and 220 m from the point of initiation of the profile.

4.3.1.13 Geophysical Imaging Through Profile 14

The geophysical image along profile 14 was taken from a forest area across a footpath within the forest which is situated at the west side of Ghummanhera village (Fig. 4.16). The arrangement of the profile is along the east-west direction. The resistivity in the sub-surface material is highly variable, and it varies from 0.0765 to 230 ohm-m. The potential water bearing zone may be expected in between 19 and 47 m depth below ground level. The groundwater quality is anticipated to be very poor because of very low resistivity of the water bearing layers. The salinity level increases after 200 m distance from the start of the profile. This poor quality of groundwater is also evidenced from the hydro-chemical data. A high resistivity value is observed near the surface which may be either a coarse texture soil or a layer of calcium carbonate, but the secondary data revealed that it is due to the surface soil of coarse textured.

4.3.1.14 Geophysical Imaging Through Profile 15

The geophysical image along profile 15 was laid in a fallow land along with a road which is situated at the side of a big village pond in the northern part of the village Chhawala (Fig. 4.17). The arrangement of the profile is of north-east and south-west direction. The resistivity in the profile is somewhat low and varies from 0.0762 to 104 ohm-m. The depth of geological layers where groundwater can be available was found at a depth of 20 to 35 m below ground level. The groundwater quality of this layer seemed to be very poor as envisaged from the observed very low resistivity value of this layer. The hydro-chemical data is also confirming the same. A highly saline pollution plume is present nearly 200 m away from the start of the profile.

4.3.1.15 Geophysical Imaging Through Profile 16

The geophysical image along profile 16 was laid on a farmer's field situated at the western side of an orchard in the northern part of the village Hasanpur (Fig. 4.18). The profile is arranged along a village road of north-south direction. The resistivity value in the profile varies between 13 and 57 ohm-m. The water bearing geological layers are expected at a depth of 30 to 45 m below ground level. The low resistivity values at the water bearing layers are telling that the quality of water stored in those layers is moderate, and this is confirmed by the hydro-chemical data obtained from those layers. Above the water potential zone, a clay-enriched layer has been found which may be formed at the time of formation of sedimentary rocks at the ancient times.

4.3.1.16 Geophysical Imaging Through Profile 17

The geophysical image along profile 17 was taken from a farmer's field situated at the side of the main road in the eastern part of the village Dhansa (Fig. 4.19). The profile is arranged along the road at east-west direction. The resistivity value of the sub-surface geological materials within the profile varies from 14 to 52 ohm-m. The expected aquifer depth in this area is about 20 m below ground level. At deeper depth (>35 m below ground level) *kankar* and clay-enriched layer is expected as inferred from their resistivity value within the profile.

4.3.1.17 Geophysical Imaging Through Profile 18

The geophysical image of profile 18 was taken from a farmer's field which is located along the main road at the north-eastern part of the village Kanganheri (Fig. 4.20). The profile is arranged at the north-south direction. The overall resistivity value of the sub-surface geological materials in the profile is very low, and the same is ranging between 0.822 and 3.57 ohm-m. The water bearing geological formations are observed at a depth of 25 to 40 m below ground level. Very low observed resistivity of the water bearing layers indicates the quality of groundwater seems to be very poor. Groundwater is situated in the unconfined aquifer, and capillary rise of water to the upper part of the vadose zone is the main cause of soil salinity in this area. The hydrostatic pressure of the aquifer also helped in this process to raise soil salinity.

4.3.2 Iso-resistivity Contours

The apparent resistivity (ρ_a) values have been interpreted using RES2DINV software. Then the localized model was generated for getting true resistivity data (h_n and ρ_n). Altogether five geophysical layers have been obtained based on Lund imaging data. The true resistivity values were interpreted, and iso-resistivity contours of these geophysical layers were mapped.

4.3.2.1 Geophysical Layer 1

The first geophysical layer varies from the surface to 7 m bgl. Resistivity values vary widely from 7 to 190 ohm-m. The iso-resistivity map of this layer is shown in Fig. 4.21. From low to high, the resistivity values of this layer are classified in to five classes, namely, <10, 10–20, 20–30, 30–40, and > 40 ohm-m. The resistivity class of <10 ohm-m indicates the presence of fine textured materials like clay. Low resistivity areas are found nearby Chhawala and Surkhpur villages. Resistivity class

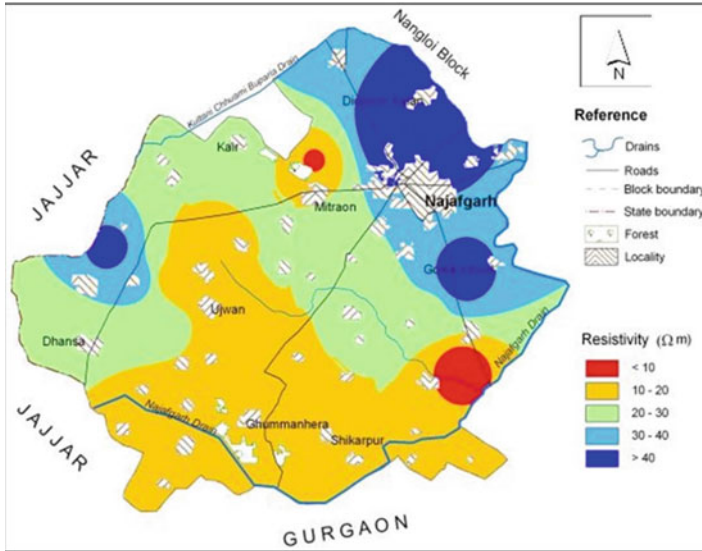


Fig. 4.21 Spatial variation of resistivity of the upper part of the sub-surface (0–7 m bgl) showing the moisture distribution pattern in the vadose zone of the study area

of 10–20 ohm-m indicates the moist soil with some amount of salts and has been located at the southern portion of the study area covering nearly 30% of the total area. The resistivity range of 30–40 ohm-m indicates moist soil and is located in the western, northern, and the middle portion of the study area. Next two ranges of resistivity values indicate relatively dry soil and predominantly found at the north and west side of the study area. Therefore, the first geophysical layer tells about the spatial pattern of soil moisture within the study area.

4.3.2.2 Geophysical Layer 2

The second geophysical layer varies from a depth of 7–15 m bgl. The variation of resistivity value of this layer is of similar magnitude of the first layer. It varies from 7 to 173 ohm-m (Fig. 4.22). This layer is also classified as that of the first layer. It has been observed that fine textured materials like clay along with some moisture are the dominating materials of the south and south eastern part of the study area covering the villages Ghummanhera and Ujwah. The resistivity values and its pattern of this layer are the typical signature of the unsaturated zone. This layer is mainly dominated by sand and *kankar* as the geologic material. Capillary movement of water is there in this layer but this layer does not store groundwater.

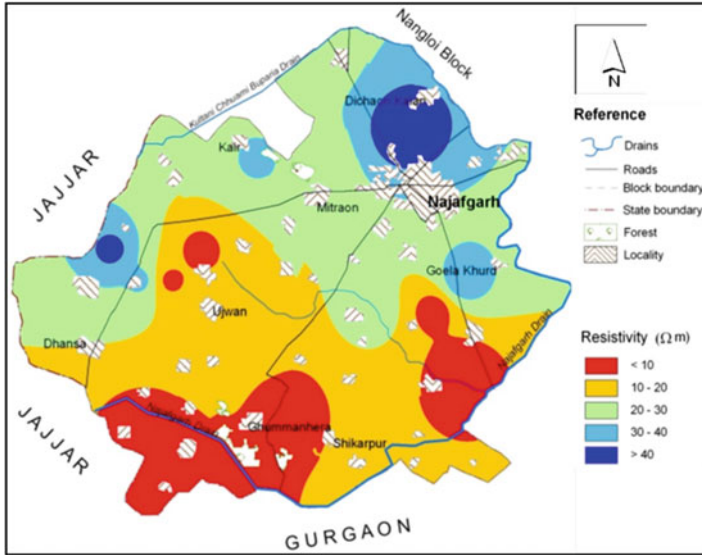


Fig. 4.22 Spatial variation of resistivity at the second geophysical layer of the sub-surface (7–15 m bgl) showing the presence of sand and *kankar* as the geologic material

4.3.2.3 Geophysical Layers 3 and 4

The geophysical layer 3 varies from 15 to 28 m bgl and the layer 4 varies from 28 to 40 m bgl. Although these are two separate layers, considering the widespread overlapping of the resistivity values of these two layers, these layers have been discussed together (Figs. 4.23 and 4.24). The zones of low resistivity value (<10 ohm-m) represent saline groundwater. The slightly low resistivity values (10–20 ohm-m) indicate the presence of water with clay. The zones of medium resistivity values (20–30 ohm-m) represent the presence of water with sand and clay. Presence of groundwater along with sand can be represented by the resistivity values of 30–40 ohm-m. In zones where high resistivity values (>40 ohm-m) are there, groundwater is available in the sand and gravelly aquifer material. Water bearing layers with better availability of groundwater mainly are formed by sand and gravel. Therefore, it may be inferred that the areas adjoining Goela Khurd village, surrounding Bagargarh village, and areas north of Jharoda Kalan village and Kair village are expected to get good amount of groundwater. As a whole, moderate quality of groundwater is expected at some pockets of north, west, and east side of the study area.

The fifth geophysical layer contains the geological materials with high resistivity values in major parts of the study area. This may represent the presence of calcite and other types of bed rock formation.

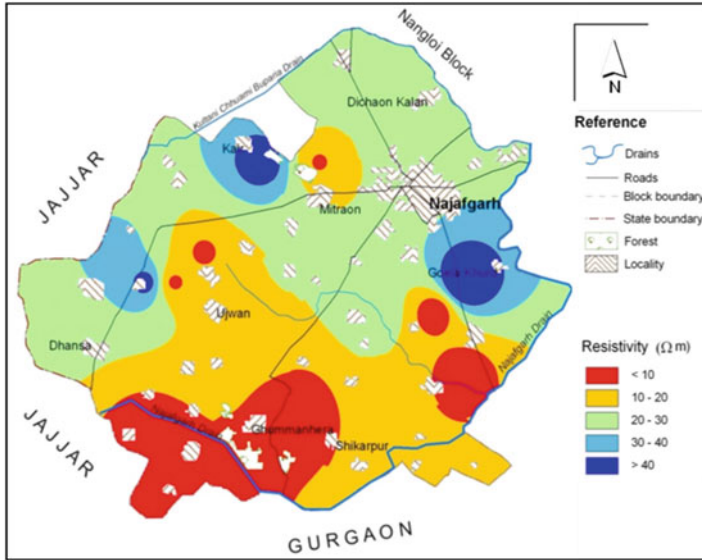


Fig. 4.23 Spatial variation of resistivity at the third geophysical layer of the sub-surface (15–28 m bgl) showing the presence of groundwater

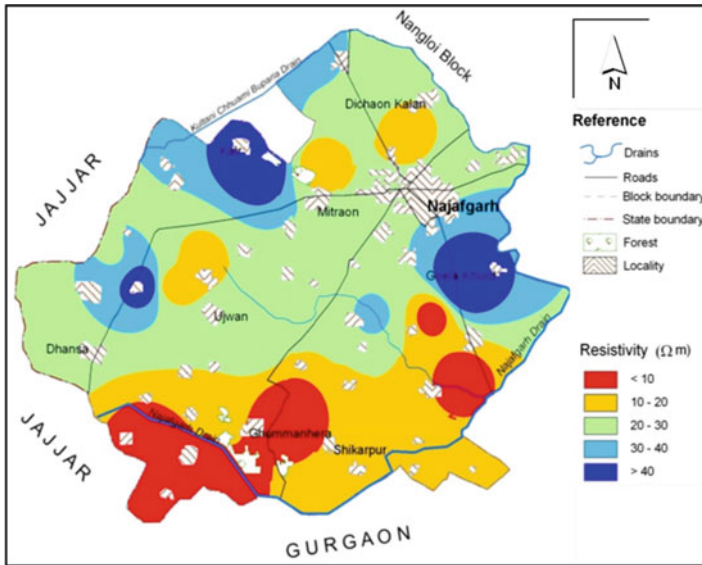


Fig. 4.24 Spatial variation of resistivity at the fourth geophysical layer of the sub-surface (28–40 m bgl) showing the presence of sand and gravel as the geologic material

4.3.3 Delineation of Water Potential Zones

For better assessment of potential groundwater zones in the study area along with true resistivity data, Dar Zarrouk parameters (S and T parameters) were used. True resistivity data (combining resistivity and thickness) of each geophysical image was interpreted, and the corresponding values of longitudinal unit conductance (S) and transverse unit resistance (T) parameters for each geophysical image were computed. The spatial distributions of these two parameters were mapped using geostatistical wizard of Arc GIS® 10.2 package.

Spatial variation map of S parameter is shown in Fig. 4.25. The S parameter was divided into five classes, and the classification scheme of S parameter with regard to the present study area is S values 0–0.5 dS (very low), 0.5–1.0 dS (low), 1.0–2.0 dS (medium), 2.0–5.0 dS (high), and > 5.0 dS (very high). It has been observed that in the study area very low and low classes of S parameter are distributed in a scattered manner. In few pockets (geophysical imaging locations of 2, 4, 5, and 17) low and very low S parameter values are observed. Higher values of S parameter (1.0–2.0, 2.0–5.0, and > 5.0 dS) cover a major portion of the study area. Spatial location of the S parameter in the range of 1.0–2.0 dS is predominantly concentrated in a strip spreading at the north side of the study area and in few selected places at the middle part of the study area, and the S parameter in the range of 2.0–5.0 dS is observed in a strip spreading at the middle portion of the study area where S parameter >5.0 dS is observed at the southern portion of the study area.

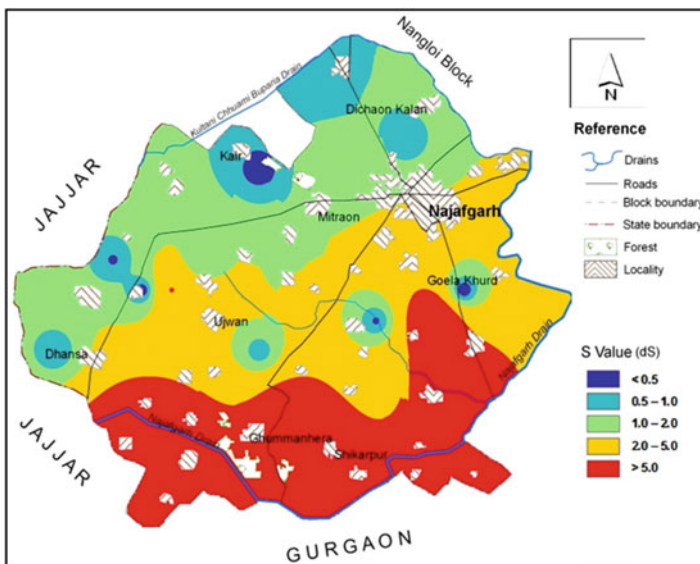


Fig. 4.25 Spatial map showing the variation of longitudinal unit conductance (S) of the groundwater in the study area

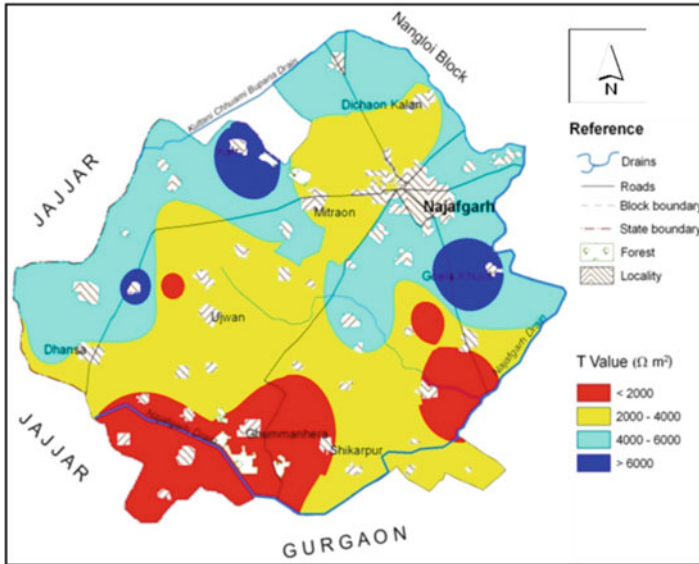


Fig. 4.26 Spatial map showing the variation of transverse unit resistance (T) of the groundwater in the study area

Spatial map of T parameter (Fig. 4.26) has been prepared taking the range of $<2000\ \text{ohm}\cdot\text{m}^2$, $2000\text{--}4000\ \text{ohm}\cdot\text{m}^2$, $4000\text{--}6000\ \text{ohm}\cdot\text{m}^2$, and $> 6000\ \text{ohm}\cdot\text{m}^2$. So, there are four classes of T parameter. It has been found that medium values of T parameter, i.e., in the range of $2000\text{--}4000\ \text{ohm}\cdot\text{m}^2$ and $4000\text{--}6000\ \text{ohm}\cdot\text{m}^2$, cover a major part of the study area. T value of $<2000\ \text{ohm}\cdot\text{m}^2$ is practically concentrated at the southern part of the study area.

A combination of Dar Zarrouk parameters (S and T parameters) has been widely used to delineate potential water bearing layers in the sub-surface. Chandra and Athavale (1979) studied various combinations of Dar Zarrouk parameters and concluded that the combination of high T and low S will be the indicator of potential water bearing layers in the sub-surface, provided that the spatial variations of water quality in that region remain more or less uniform. Transmissivity ($T_r = K \cdot b$; K, hydraulic conductivity; b, aquifer thickness) of the aquifer and transverse unit resistance (T) can also be used to identify potential aquifer, and the relationship between these two is linear (Kelley 1977). As the transmissivity is directly related to the characteristics of the aquifer, T parameter indirectly shows water potential zones. Keeping all these findings the criteria table as proposed by Adhikary et al. (2012) (Table 4.1) has been followed to classify the area in terms of high, moderate, and poor water potential zones. Based on this criteria table these two thematic maps (S and T) were overlaid to get the combination of S and T parameters (Fig. 4.27), which will directly show the hotspots where we can expect better groundwater.

Table 4.1 Criteria table by using different combinations of Dar Zarrouk parameters for delineating water potential zones (Adhikary et al. 2012)

S parameter (dS)	T parameter (Ω meter ²)	Category
1.0–2.0	<2000	2 (moderate)
	2000–4000	1 (good)
	>4000	1 (good)
2.0–5.0	<2000	3 (poor)
	2000–4000	2 (moderate)
	>4000	1 (good)
>5.0	<2000	3 (poor)
	2000–4000	3 (poor)
	>4000	2 (moderate)

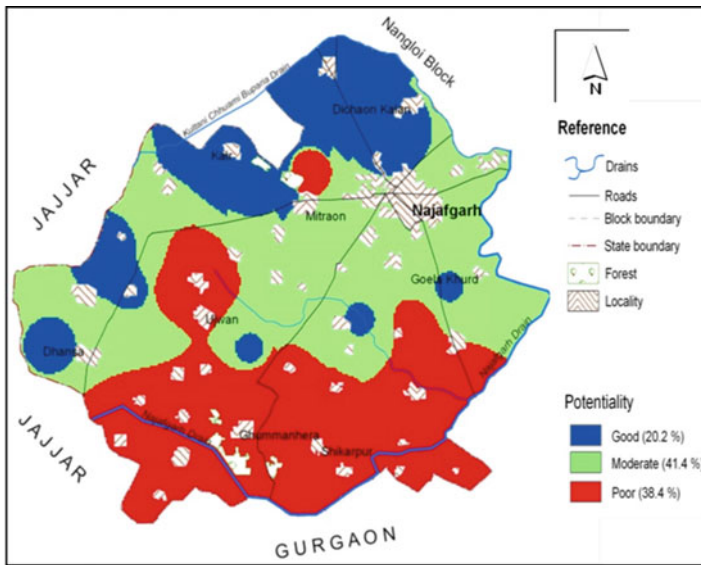


Fig. 4.27 Overlay map of S and T parameters indicating potential groundwater zones of the study area

In the study area better water potential zones are found at the north side covering the villages Dichaon Kalan, Kair, etc. In few pockets at the west side of study area, good amount of water is also available. Poor water potential zones are mainly concentrated at the southern border of the study area where Najafgarh drain is flowing. Area wise it has been observed that nearly 41.4% of the study area is coming under moderate water potential zones. In 38.4% of the area poor water potentiality has been observed, and only 20.2% of the area is having good water potentiality. Therefore, for sustainable vegetable cultivation, rain water harvesting and consumptive use of surface and groundwater may be adopted.

4.4 Conclusion

In this study geophysical imaging technique has been proved as an effective technique to delineate the sub-surface configuration. The geophysical investigation reveals that the potential groundwater zones are expected at a depth of 20–30 m below ground level. On spatial scale good groundwater potential zones are mainly found at the north and west side of Najafgarh covering 20.1% of the study area. Bagargarh, Ghasipura, Goela Khurd, Jharoda Kalan, and Kair are the few villages where intensive vegetable cultivation may be possible because of availability of good amount of groundwater. The groundwater quality of the study area is moderate to poor, and poor-quality zones are mainly found in the villages Ghummanhera and Ujwah. For sustainable vegetable production, rain water harvesting and consumptive use of surface and groundwater may be adopted.

References

- Adhikary, P.P., Chandrasekharan, H., Chakraborty, D., Kamble, K. (2010). Assessment of groundwater pollution in west Delhi, India using geostatistical approach. *Environmental Monitoring and Assessment* 167:599-615.
- Adhikary, P.P., Chandrasekharan, H., Chakraborty, D., Kumar, B., Yadav, B.R. (2009). Statistical approaches for hydrogeochemical characterization of groundwater in West Delhi, India. *Environmental Monitoring and Assessment* 154:41-52.
- Adhikary, P.P., Dash, C.J., Chandrasekharan, H., Rajput, T.B.S., Dubey, S.K. (2012). Evaluation of groundwater quality for irrigation and drinking using GIS and geostatistics in a peri-urban area of Delhi, India. *Arabian Journal of Geosciences* 5:1423-1434.
- Adhikary, P.P. and Biswas, H. (2011). Geospatial assessment of groundwater quality in Datia district of Bundelkhand. *Indian Journal of Soil Conservation* 39(2): 108-116.
- Adhikary, P.P., Chandrasekharan, H., Dash, C.J., Jakhar, P. (2014a). Integrated isotopic and hydrochemical approach to identify and evaluate the source and extent of groundwater pollution in west Delhi, India, *Indian Journal of Soil Conservation* 42 (1), 17-28.
- Adhikary, P.P., Chandrasekharan, H., Dash, C.J., Kumar, G. (2015c). Hydrogeochemical investigation of groundwater quality in west Delhi, India, *Indian Journal of Soil Conservation* 43 (1), 15-23.
- Adhikary, P.P., Chandrasekharan, H., Dubey, S.K., Trivedi, S.M., Dash, C.J. (2015a). Electrical resistivity tomography for assessment of groundwater salinity in west Delhi, India, *Arabian Journal of Geosciences* 8 (5), 2687-2698.
- Adhikary, P.P., Chandrasekharan, H., Trivedi, S.M., Dash, C.J. (2015b). GIS applicability to assess spatio-temporal variation of groundwater quality and sustainable use for irrigation, *Arabian Journal of Geosciences* 8 (5), 2699-2711.
- Adhikary, P.P., Dash, C.J. (2017). Comparison of deterministic and stochastic methods to predict spatial variation of groundwater depth, *Applied Water Science* 7 (1), 339-348.
- Adhikary, P.P., Dash, C.J., Bej, R., Chandrasekharan, H. (2011). Indicator and probability kriging methods for delineating Cu, Fe, and Mn contamination in groundwater of Najafgarh Block, Delhi, India, *Environmental Monitoring and Assessment* 176 (1-4), 663-676.
- Adhikary, P.P., Dash, C.J., Sarangi, A., Singh, D.K. (2014b). Hydrochemical characterization and spatial distribution of fluoride in groundwater of Delhi state, India. *Indian Journal of Soil Conservation* 42 (2), 170-173.

- Ahmadi SH, Sedghamiz A (2008) Application and evaluation of kriging and cokriging methods on groundwater depth mapping. *Environmental Monitoring and Assessment* 138:357–368.
- Al Gami MA (2011) Magnetic and DC resistivity investigation for groundwater in a complex subsurface terrain. *Arabian Journal of Geosciences* 4:385–400.
- Arslan H (2014) Estimation of spatial distribution of groundwater level and risky areas of seawater intrusion on the coastal region in Çarşamba Plain, Turkey, using different interpolation methods. *Environmental Monitoring and Assessment* doi:<https://doi.org/10.1007/s10661-014-3764-z>.
- Bhattacharya, R.K. and Patra, H.P. (1968). *Direct current geoelectric sounding*. Elsevier Publishing Co., Amsterdam, pp. 135.
- Burgess TM, Webster R (1980) Optimal interpolation and isarithmic mapping of soil properties I: The semivariogram and punctual kriging. *Journal of Soil Science* 31:315-331.
- CGWB (1996) Development and augmentation of groundwater resources in National Capital Territory of Delhi. Ministry of Water Resources, Government of India 42p.
- Chandra, P.C. and Athavale, R.N. (1979). Close grid resistivity survey for demarcating the aquifer encountered in bore well at Koyyur in lower Maner basin. Tech. Report No. GH-11-Gp-7, Hyderabad, pp. 16.
- Dash JP, Sarangi A, Singh DK (2010) Spatial variability of groundwater depth and quality parameters in the National Capital Territory of Delhi. *Environmental Management* 45(3):640-650.
- De Grooth-Hedlin C, Constable S (1990) Occm's inversion to generate smooth, two-dimensional models from magneto-telluric data. *Geophysics* 55:1613-1624.
- Dorbin, M.B. (1960). *Introduction to geographical prospecting*. McGraw Hill Book Co., pp. 466.
- Edwards, L.S. (1977). A modified pseudosection for resistivity and induced polarization. *Geophysics*, 42: 1020-1036.
- Griffiths DH, Barker RD (1993) Two-dimensional resistivity imaging and modeling in areas of complex geology. *Journal of Applied Geophysics* 29:211–226.
- IMD (1991). *Climate of Haryana and Union Territories of Delhi and Chandigarh*. India Meteorological Department, Govt. of India Report. pp. 92-98.
- Isaaks EH, Srivastava RM (1989) *An Introduction to Applied Geostatistics*. Oxford University, New York.
- Kelley, W.E. (1977). Geo-electric sounding for estimating aquifer hydraulic conductivity. *Ground Water*, 15(6): 420-425.
- Loke MH, Barker RD (1996) Rapid least-squares inversion of apparent resistivity pseudo sections by a quasi-Newton method. *Geophysical Prospect* 44:499–524.
- Mazac O, Kelly WE, Landa I (1987) Surface geo-electrics for ground water pollution and protection studies. *Journal of Hydrology* 93:277-294.
- Nikroo L, Kompani-Zare M, Sepaskhah A, Fallah Shamsi S (2010) Groundwater depth and elevation interpolation by kriging methods in Mohr Basin of Fars province in Iran. *Environmental Monitoring and Assessment* 166(1–4):387–407.
- Prakash MR, Singh VS (2000) Network design for groundwater monitoring – A case study. *Environmental Geology* 39:628–632.
- Prasanna, M.V., Chidambaram, S., Senthil Kumar, G., Ramanathan, A.L. and Nainwal, H.C. 2011. Hydrogeochemical assessment of groundwater in Neyveli Basin, Cuddalore District, South India, *Arabian Journal of Geosciences* 4: 319–330.
- Rao VVSG, Rao GT, Surinaidu L, Rajesh R, Mahesh J (2011) Geophysical and Geochemical Approach for Seawater Intrusion Assessment in the Godavari Delta Basin, A.P., India. *Water Air and Soil Pollution* 217:503–514.
- Sasaki Y (1992) Resolution of resistivity tomography inferred from Numerical Simulation. *Geophysical Prospect* 40: 453–464.
- Sen, N. (1952). Geomorphological evaluation of Delhi area. *Current Science*, 21: 157-159.
- Skuthan B, Mazac O, Landa I (1986) The importance of geophysical methods for protecting ground water from agricultural pollution. *Proc. J. Geol. Sci., Sect. Appl. Geophys* 11:27-39.

- Sun Y, Kang S, Li F, Zhang L (2009) Comparison of interpolation methods for depth to groundwater and its temporal and spatial variations in the Minqin oasis of Northwest China. *Environmental Modelling and Software* 24:1163-1170.
- Theodossiou N, Latinopoulos P (2006) Evaluation and optimization of groundwater observation networks using the kriging methodology. *Environmental Modelling and Software* 21:991-1000.
- Ustra AT, Elis VR, Mondelli G, Zuquette LV, Giacheti HL (2012) Case study: a 3D resistivity and induced polarization imaging from downstream a waste disposal site in Brazil. *Environmental Earth Sciences* 66:763-772.
- Varouchakis EA, Hristopulos DT (2013) Comparison of stochastic and deterministic methods for mapping groundwater level spatial variability in sparsely monitored basins. *Environmental Monitoring and Assessment* 185:1-19.
- Verma, R.K., Rao, M.K. and Rao, C.V. (1980). Resistivity investigations for ground water in metamorphic area near Dhanbad, India. *Ground Water*, 18: 46-55.